On the time required to establish chemical and isotopic equilibrium in the carbon dioxide system in seawater

Richard E. Zeebe [*], D.A. Wolf-Gladrow, H. Jansen

Alfred Wegener Institute for Polar and Marine Research, Postfach 12 01 61, D-27515 Bremerhaven, Germany

Abstract

Dissolved inorganic carbon in sea water plays a key role in understanding the properties of the oceanic carbon reservoir within the global carbon cycle. For instance, fluxes between the atmosphere and the ocean are estimated using the stable carbon isotopes ^{12}C and ^{13}C of atmospheric CO_2 and its dissolved forms within the ocean. Likewise, the investigation of carbon uptake by marine phytoplankton or the reconstruction of past oceans via stable isotope analysis demand a sound understanding of the sea water chemistry and associated carbon isotope fractionation. Chemical and isotopic disequilibrium is of particular interest when small length and time scales are considered. For example, within the microenvironment of marine plankton or within the surface boundary layer of the ocean (gas exchange atmosphere-ocean) the seawater carbonate chemistry deviates appreciably from equilibrium. It can be shown that a time-dependent description of the carbonate system is indispensable when time scales smaller than 90 s are involved (length scale of the diffusive boundary layer $\sim 10^{-4}$ m). Properties of the equilibrium state of the carbonate system in sea water are well known. However, hitherto there is little detailed work on the disequilibrium state of the chemical and in particular on the isotopic properties of the system. Here we present analytical and numerical techniques to determine the relaxation time of the chemical system including $^{\nu}CO_2, H^{\nu}CO_3^-, ^{\nu}CO_3^{2-}$, H^+, OH^-, $B(OH)_3$, and $B(OH)_4^-$, where $\nu = 12$, 13, and 14. The calculated relaxation time for chemical equilibrium at a temperature of 25°C and a salinity of 35 at pH 8.2 is 15.9 s (only ^{12}C species), while the time calculated for isotopic equilibrium is 17.5 s (all carbon isotopes considered). © 1999 Elsevier Science B.V. All rights reserved.

Keywords: seawater; chemical and isotopic equilibrium; carbon dioxide system

1. Introduction

A detailed understanding of the carbon dioxide system in seawater is a prerequisite for the investigation of a variety of phenomena in the marine environment. For example, the storage capacity of the ocean for anthropogenic CO_2 is limited by the buffer properties of the seawater chemistry (so called 'Revelle' factor (for review see, e.g., Siegenthaler, 1993; Stumm and Morgan, 1996)). Another example of the role of sea water

---

[*] Corresponding author. Tel.: +49-471-4831-812; Fax: +49-471-4831-425; E-mail: rzeebe@awi-bremerhaven.de

chemistry in the global carbon cycle is the CO_2 exchange between ocean and atmosphere. The chemical state of the ocean and particularly the fluctuations of the ocean chemistry between glacial and interglacial periods are crucial for the atmospheric CO_2 content on this time scale (e.g., Broecker and Peng, 1993; Archer and Maier-Reimer, 1994).

While a description by equilibrium properties is reasonable for most of the mentioned phenomena an analogous treatment of processes on small time and length scales is inadequate. On small length scales (diffusive boundary layer $\leq 10^{-2}$ m) where the transport or the supply of chemical substances is not governed by advection or turbulent mixing (Lazier and Mann, 1989), chemical conversion and diffusion are the dominant mechanisms. The characteristic time scale of diffusion can be estimated by $\tau = l^2/D$, where l is the length scale (m) of the boundary layer and $D \approx 10^{-9}$ m^2 s^{-1} is the diffusion coefficient of the dissolved chemical species. With the typical length scale of the diffusive boundary layer of gas exchange at the ocean-atmosphere interface ($0.3-1.5 \times 10^{-4}$ m (Emerson, 1995)) or of larger marine plankton such as aggregates or foraminifera (3×10^{-4} m (Wolf-Gladrow et al., 1999)) one obtains a characteristic time scale of 1–90 s. Since the establishment of chemical equilibrium is of the same order of magnitude (as will be shown in this paper) processes faster than this cannot be adequately described by a time-independent consideration.

An example of the use of time-dependent descriptions of the carbonate system is the identification of sources of inorganic carbon for photosynthesis by marine phytoplankton via isotopic disequilibrium technique (Lehman, 1978; Korb et al., 1997). This technique compares the theoretically calculated relaxation time with the measured photosynthetic uptake of radiocarbon as a function of time to distinguish between CO_2 and HCO_3^- uptake in marine diatoms. Thus, the relaxation time derived in this paper can be used to address a long-debated question concerning the inorganic carbon acquisition in marine phytoplankton. Where stable oxygen isotopes are concerned, disequilibrium properties may also help in comprehending nonequilibrium fractionations in synthetic carbonates (cf. Kim and O'Neil, 1997).

Moreover, disequilibrium of the carbonate system might subtly affect the interpretation of paleoceanographic records found in marine sediments. Spero et al. (1997) recently found that the sea water chemistry affects the stable carbon and oxygen isotope fractionation in the calcite shells of foraminifera, which provide an important tool in paleoceanography. Zeebe et al. (1999) applied a diffusion–reaction model to the microenvironment of foraminifera to show that this effect can be understood to a large degree in terms of an interaction between the sea water chemistry and the life processes of the organisms. However, some discrepancies between the model and observations remain and it is suggested that during the calcification process a mechanism is active which depends on the rate of calcite precipitation (first proposed by McCrea, 1950). Thus, a refined description of the incorporation of stable carbon and oxygen isotopes into the calcite lattice demands a time dependent model of the chemical environment which involves a disequilibrium of the fluxes and of the carbonate system. An important step towards this approach is a model of the response of a disturbed chemical system as a function of time (disequilibrium with respect to time, spatially homogeneous).

A specific question that can be addressed with this model concerns the experimental determination of the primary production in seawater by the uptake of radioactive ^{14}C (e.g., Strickland and Parsons, 1968). In this method, radiocarbon (in the form of $NaH^{14}CO_3$ or $Na_2{}^{14}CO_3$) is added at a known ratio to the total dissolved inorganic carbon content of the seawater sample. The uptake of radiocarbon by phytoplankton is converted to total carbon uptake using this radiocarbon:total carbon ratio. An underlying assumption is that the chemical and isotopic equilibrium (e.g., conversion from $^{14}CO_3^{2-}$ to $H^{14}CO_3^-$, and from $H^{14}CO_3^-$ to $^{14}CO_2$, respectively) is already established. If this is not true, measurements of the primary production by the uptake of ^{14}C would yield incorrect results.

Generally, the calculations to be presented here can be used to decide whether it is reasonable to use equilibrium or disequilibrium properties of the system. Particularly, the mathematical analysis of the chemical reactions (by use of the mathematical theory of dynamical systems) should lead to a detailed understanding of the mechanisms involved. Whereas a great number of articles have been published on the equilibrium behavior of the carbonate system (e.g, Maier-Reimer and Hasselmann, 1987; DOE, 1994; Millero, 1995) the chemical

and isotopic properties of the carbonate system in disequilibrium have hitherto received little attention. Lehman (1978) and Usdowski (1982) calculated the time required for the establishment of the chemical equilibrium of the carbon dioxide system. However, their results are restricted to a simplified model that assumes instantaneous equilibrium for the protonation of CO_3^{2-} and the equilibrium of H_2O. Using this approximation, time scales smaller than seconds cannot be described adequately. In addition, boron compounds were not included in both analyses and the work by Usdowski (1982) considers a fresh water system.

In this paper, we present analytical and numerical calculations that determine the time required to establish the chemical and isotopic equilibrium of the carbon compounds of the carbon dioxide system in sea water. We take advantage of the full set of kinetic rate constants for the carbonate system (including boron) given by Wolf-Gladrow and Riebesell (1997) which enables us to analyze the system on time scales ranging from microseconds to minutes. The obtained results can be utilized for, e.g., identification of inorganic carbon sources in marine diatoms (isotope disequilibrium technique) or determination of isotope equilibration times in measurements of primary production. Particularly, a further development of the presented model (including chemical and isotopic disequilibrium processes within the vicinity of a growing crystal) should help to understand nonequilibrium fractionation in synthetic and biogenic carbonates.

2. Analytical and numerical calculations

The results of the following calculations might indeed be of practical interest for biologists or geochemists — the way to obtain these results is, however, rather theoretical. The description of the time development of the chemical species of the carbonate system leads to a set of ordinary differential equations of first order, and can therefore be analyzed by the mathematical theory of dynamical systems.

2.1. Decoupled reactions of CO_2 and H_2O

To demonstrate the technique of the determination of relaxation constants of a chemical system, a highly simplified system is considered first: the hydration of CO_2 and the reaction of H_2O, OH^-, and H^+. In this section these reactions will be analyzed separately and decoupled from any other reaction of the carbonate system. The coupling of both reactions is examined in Section 2.2, whereas the complete system (including boron) will be solved numerically in Section 2.3.

2.1.1. Hydration of CO_2

The hydration of CO_2 is described by the following reaction:

$$CO_2 + H_2O \underset{k_{-1}}{\overset{k_{+1}}{\rightleftharpoons}} H^+ + HCO_3^- \tag{1}$$

where k_{+1} and k_{-1} are the rate constants for the forward and backward reactions, respectively; see Wolf-Gladrow and Riebesell (1997) for numerical values. (If not otherwise indicated, all calculated results in this paper refer to $T = 25°C$, pH = 8.2, and $S = 35$). The rate laws for the chemical species are

$$\frac{d[CO_2]}{dt} = +k_{-1}[H^+][HCO_3^-] - k_{+1}[CO_2]$$

$$\frac{d[HCO_3^-]}{dt} = -k_{-1}[H^+][HCO_3^-] + k_{+1}[CO_2]$$

$$\frac{d[H^+]}{dt} = -k_{-1}[H^+][HCO_3^-] + k_{+1}[CO_2] \tag{2}$$

from which one can see that

$$\frac{d[CO_2]}{dt} = -\frac{d[HCO_3^-]}{dt} = -\frac{d[H^+]}{dt}. \tag{3}$$

Thus, the system of differential equations can be reduced to one equation for CO_2 because it follows from Eq. (3) that

$$[HCO_3^-] = C_0 - [CO_2]$$

and

$$[H^+] = C_1 - [CO_2]$$

where C_0 and C_1 are constants. Here, the total dissolved inorganic carbon (ΣCO_2) is the sum of HCO_3^- and CO_2 and thus $C_0 = \Sigma CO_2$. Introducing the alkalinity ($Alk = [HCO_3^-] - [H^+]$), it is obvious that $C_1 = \Sigma CO_2$-Alk. The equation for CO_2 therefore reads

$$\frac{d[CO_2]}{dt} = +k_{-1}(\Sigma CO_2 - Alk - [CO_2])(\Sigma CO_2 - [CO_2]) - k_{+1}[CO_2]. \tag{4}$$

This is a nonlinear first order equation for CO_2. To calculate the relaxation time for a small perturbation in CO_2, Eq. (4) is expanded in the vicinity of the equilibrium $[CO_2]^*$, where the equilibrium is given by (see reaction (1)):

$$\frac{[HCO_3^-]^*[H^+]^*}{[CO_2]^*} = \frac{k_{+1}}{k_{-1}}$$

Inserting $[CO_2] = [CO_2]^* + \delta CO_2$ into Eq. (4), where δCO_2 is the deviation of CO_2 from equilibrium, using $d[CO_2]^*/dt = 0$ and neglecting quadratic terms of δCO_2 one obtains

$$\delta \dot{C}O_2 = -\left[k_{+1} + k_{-1}([H^+]^* + [HCO_3^-]^*)\right]\delta CO_2 \tag{5}$$

The solution is

$$\delta CO_2 = \delta CO_2^0 \exp(-t/\tau_1)$$

where δCO_2^0 is the perturbation in CO_2 at $t = 0$, and τ_1 is given by:

$$\tau_1 = \frac{1}{k_{+1} + k_{-1}([H^+]^* + [HCO_3^-]^*)}. \tag{6}$$

A small perturbation in CO_2 therefore decreases exponentially with time constant τ_1. Given $k_{+1} = 0.036$ s^{-1}, $k_{-1} = 3.3 \times 10^4$ kg mol^{-1} s^{-1}, $[H^+]^* = 6.3 \times 10^{-9}$ mol kg^{-1}, and $[HCO_3^-]^* = 1.8 \times 10^{-3}$ mol kg^{-1}, τ_1 is 0.017 s. [1] In summary, if the hydration of CO_2 is the only reaction considered, chemical equilibrium is achieved in about two hundredth of a second.

2.1.2. Water

For the reaction between H^+, OH^-, and H_2O, namely

$$H_2O \underset{k_{-6}}{\overset{k_{+6}}{\rightleftharpoons}} H^+ + OH^- \tag{7}$$

a similar calculation yields a time constant τ_2 for the relaxation of small deviations of H^+ and OH^- from equilibrium (the notation of the rate constants for the chemical reactions follows Wolf-Gladrow and Riebesell,

---

[1] Relaxation times in this paper are calculated as the time required to achieve 37% of the initial perturbation ($\approx 1/e \times 100$). Provided that the decrease is exponential one can calculate the time to achieve 99% of the equilibrium value, which is about 4.6 ($\approx -\ln(0.01)$) times larger than the relaxation time.

1997). The change in the concentration of H_2O is negligible because the concentration of water (55.56 mol kg^{-1}) is more than 10^5 times larger than the concentrations of H^+ and OH^- ($4 < pH < 10$). The relaxation constant τ_2 is:

$$\tau_2 = \frac{1}{k_{-6}\left([H^+]^* + [OH^-]^*\right)}. \tag{8}$$

Given $k_{-6} = 2.8 \times 10^{10}$ kg mol^{-1} s^{-1}, $[H^+]^* = 6.3 \times 10^{-9}$ mol kg^{-1}, and $[OH^-]^* = 7.4 \times 10^{-6}$ mol kg^{-1}, τ_2 is 4.8×10^{-6} s. Here, this calculation is used to determine τ_2 from k_{-6}. However, to determine the value of k_{-6} from experiment the reversed approach is commonly used: τ_2 is determined from temperature jump methods and the reaction rate is calculated from the relaxation time (this is actually the way to obtain k_{-6} (Atkins, 1990)). The time required to establish an equilibrium between H^+, OH^-, and H_2O is therefore in the order of several microseconds.

2.2. Coupling of CO_2 and H_2O

From the results obtained in the previous sections one would expect that the relaxation time for the coupled chemical system (i.e., reactions (1) and (7) together) would be in the order of the slower reaction, i.e., about 0.02 s. However, we will show that the time constant of the coupled system is ca. 10 s which is about 500 times larger than the estimated relaxation time of the hydration of CO_2 in Section 2.1.1. The chemical reactions considered are:

$$CO_2 + H_2O \underset{k_{-1}}{\overset{k_{+1}}{\rightleftharpoons}} H^+ + HCO_3^- \tag{9}$$

$$H_2O \underset{k_{-6}}{\overset{k_{+6}}{\rightleftharpoons}} H^+ + OH^-. \tag{10}$$

The set of differential equations therefore reads:

$$
\begin{aligned}
\frac{d[CO_2]}{dt} &= +k_{-1}[H^+][HCO_3^-] - k_{+1}[CO_2] \\
\frac{d[HCO_3^-]}{dt} &= -k_{-1}[H^+][HCO_3^-] + k_{+1}[CO_2] \\
\frac{d[H^+]}{dt} &= -k_{-1}[H^+][HCO_3^-] + k_{+1}[CO_2] + k_{+6} - k_{-6}[H^+][OH^-] \\
\frac{d[OH^-]}{dt} &= +k_{+6} - k_{-6}[H^+][OH^-]
\end{aligned}
\tag{11}
$$

HCO_3^- and H^+ can be eliminated because

$$\frac{d[HCO_3^-]}{dt} = -\frac{d[CO_2]}{dt}$$

and

$$\frac{d[H^+]}{dt} = -\frac{d[CO_2]}{dt} + \frac{d[OH^-]}{dt}$$

and therefore

$$
\begin{aligned}
[HCO_3^-] &= \Sigma CO_2 - [CO_2] \\
[H^+] &= C_2 - [CO_2] + [OH^-]
\end{aligned}
$$

with $C_2 = \Sigma CO_2 - Alk$ (note that $Alk = [HCO_3^-] + [OH^-] - [H^+]$ in this case). The equations for CO_2 and OH^- then read:

$$R_{CO_2} \quad := \quad \frac{d[CO_2]}{dt}$$

$$\qquad = \quad +k_{-1}(\Sigma CO_2 - [CO_2])(\Sigma CO_2 - Alk - [CO_2] + [OH^-]) - k_{+1}[CO_2] \tag{12}$$

$$R_{OH^-} \quad := \quad \frac{d[OH^-]}{dt}$$

$$\qquad = \quad +k_{+6} - k_{-6}(\Sigma CO_2 - Alk - [CO_2] + [OH^-])[OH^-] \tag{13}$$

The behavior of this dynamical system in the vicinity of the equilibrium is described by:

$$\begin{pmatrix} d(\delta CO_2)/dt \\ d(\delta OH^-)/dt \end{pmatrix} = \begin{pmatrix} \delta \dot{C}O_2 \\ \delta \dot{O}H^- \end{pmatrix} = \mathscr{D}|_* \begin{pmatrix} \delta CO_2 \\ \delta OH^- \end{pmatrix} \tag{14}$$

where δCO_2 and δOH^- are small deviations from equilibrium, and $\mathscr{D}|_*$ is the Jacobian of Eqs. (12) and (13) at equilibrium:

$$\mathscr{D}|_* \quad = \quad \begin{pmatrix} \left.\dfrac{\partial R_{CO_2}}{\partial [CO_2]}\right|_* & \left.\dfrac{\partial R_{CO_2}}{\partial [OH^-]}\right|_* \\[2ex] \left.\dfrac{\partial R_{OH^-}}{\partial [CO_2]}\right|_* & \left.\dfrac{\partial R_{OH^-}}{\partial [OH^-]}\right|_* \end{pmatrix}$$

$$\qquad = \quad \begin{pmatrix} -\left[k_{+1} + k_{-1}([H^+]^* + [HCO_3^-]^*)\right] & +k_{-1}[HCO_3^-]^* \\[2ex] +k_{-6}[OH^-]^* & -k_{-6}([H^+]^* + [OH^-]^*) \end{pmatrix} \tag{15}$$

or introducing the relaxation times of the decoupled reactions:

$$\mathscr{D}|_* = \begin{pmatrix} -1/\tau_1 & k_{-1}[HCO_3^-]^* \\ k_{-6}[OH^-]^* & -1/\tau_2 \end{pmatrix} \tag{16}$$

The eigenvalues $\lambda^{a,b}$ of $\mathscr{D}|_*$ determine the behavior of the coupled system:

$$\lambda^{a,b} = -\frac{1/\tau_1 + 1/\tau_2}{2} \pm \sqrt{\left(\frac{1/\tau_1 + 1/\tau_2}{2}\right)^2 - \frac{1}{\tau_1 \tau_2} + k_{-1}k_{-6}[HCO_3^-]^*[OH^-]^*} \;. \tag{17}$$

The time constants are given by the inverse of the eigenvalues. Using the numerical values stated above, one obtains:

$$\tau_3^a \quad = \quad -1/\lambda^a \quad = \quad 11.5\,s$$

$$\tau_3^b \quad = \quad -1/\lambda^b \quad = \quad 4.8 \times 10^{-6}\,s$$

Thus, the coupled system exhibits two extremely different relaxation times. Such equations are called 'stiff'. This property is expressed by the ratio of the largest and the smallest eigenvalue which gives 2.4×10^6. It should be emphasized that the relaxation time of the entire chemical system is given by the slowest process and is therefore of the order of 10 s. Remark: the behavior of the linearized system (14) can be deduced from the eigenvalues alone, therefore the exact solution (see Appendix B) was not discussed here.

2.2.1. Chemical background

A priori it is not clear why the coupled chemical system takes such a long time to achieve equilibrium, particularly, because each of the single reactions relaxes faster ($\approx 10^{-6}$ and 0.02 s). This phenomenon can be explained by examining the time evolution of a small perturbation in CO_2. For the decoupled reaction the relaxation of δCO_2 is given by:

$$\delta \dot{C}O_2 = -(1/\tau_1)\,\delta CO_2$$

where τ_1 is positive, which means that a perturbation in CO_2 is exclusively damped exponentially. For the coupled system the time evolution of δCO_2 can be written as:

$$\delta \dot{C}O_2 = -(1/\tau_1)\,\delta CO_2 + k_{-1}[HCO_3^-]^*\,\delta OH^-. \tag{18}$$

In this case, a perturbation in CO_2 is damped by the first term $(-(1/\tau_1)\,\delta CO_2)$ in Eq. (18) but amplified by the second term $(+k_{-1}[HCO_3^-]^*\,\delta OH^-)$. Since the influence of the dampening term is slightly higher than the influence of the amplifying term the overall time development results in a slow relaxation of the system. The coupled system therefore exhibits a much larger relaxation time than the decoupled reactions. The chemical mechanism can be described as follows: A conversion of CO_2 to HCO_3^- results in a release of H^+. The production of hydrogen ions, however, is not arbitrary since the alkalinity must be conserved during this process. The coupling therefore slows down the conversion from carbon dioxide to bicarbonate.

Further information can be deduced by examining the eigenvectors of the Jacobian at equilibrium. The time evolution of a small deviation from equilibrium is given by (see Eq. (14)):

$$\begin{pmatrix} \delta \dot{C}O_2 \\ \delta \dot{O}H^- \end{pmatrix} = \mathscr{D}|_* \begin{pmatrix} \delta CO_2 \\ \delta OH^- \end{pmatrix}$$

which means that the perturbations (δCO_2 and δOH^-) are mapped by the matrix $\mathscr{D}|^*$ to yield the changes in time of these components ($\delta \dot{C}O_2$ and $\delta \dot{O}H^-$). The eigenvectors $\vec{u}$ and $\vec{v}$ of $\mathscr{D}|^*$ are defined such that their direction is invariant when mapped by $\mathscr{D}|^*$ (only the length changes), for instance:

$$\mathscr{D}|_*\,\vec{u} = \lambda^a \vec{u}$$

where λ^a is the corresponding eigenvalue to eigenvector $\vec{u}$. The numerical values of the eigenvalues and normalized eigenvectors at pH 8.2 are:

$$\lambda^a = -0.087; \qquad \vec{u} = \begin{pmatrix} 0.7074 \\ 0.7068 \end{pmatrix}$$

$$\lambda^b = -2.1 \times 10^5; \qquad \vec{v} = \begin{pmatrix} -2.88 \times 10^{-4} \\ 1 - 4.155 \times 10^{-8} \end{pmatrix} \approx \begin{pmatrix} 0 \\ 1 \end{pmatrix}.$$

The eigenvectors and the vector field ($\delta \dot{C}O_2$, $\delta \dot{O}H^-$) in the vicinity of the equilibrium are shown in Fig. 1. The equilibrium is at the origin of the coordinate system ($\delta CO_2 = \delta OH^- = 0$). The first eigenvector $\vec{u}$ is nearly parallel to the diagonal; the angle between the δCO_2 axis and the first eigenvector is $\approx 45°$. The second eigenvector $\vec{v}$ is nearly parallel to the δOH^- axis. Thus, the system has two eigenvectors which are not orthogonal to one another.

The time development of the components can be seen by following the arrows. Initializing the deviation from equilibrium (δCO_2, δOH^-) = (0.6, 0.1) μmol kg^{-1} as indicated by the dashed line, the system jumps to a higher OH^- concentration within 10^{-6} s along the direction $\vec{v}$. This is approximately the time required to establish a 'near-equilibrium state' between H^+ and OH^- (the product of $[OH^-]$ and $[H^+]$ is nearly constant
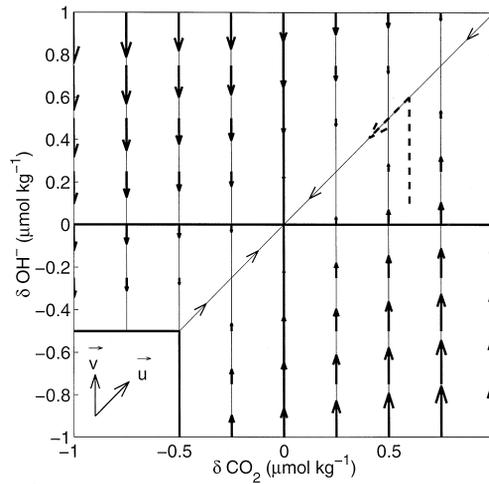
Fig. 1. The vector field $(\delta \dot{C}O_2, \delta \dot{O}H^-)$ in the vicinity of the equilibrium of the coupled system. The origin of the coordinate system represents the equilibrium concentrations. The vectors define the velocity field corresponding to the time development of the chemical reactions. The eigenvectors $\vec{u}$ and $\vec{v}$ are not orthogonal to one another (left lower corner). The streamlines of the vector field are indicated by the thin lines, whereas the dashed arrow shows the development of a perturbation in OH^- and CO_2 with initial values $(\delta CO_2, \delta OH^-) = (0.6, 0.1)$ μmol kg^{-1}.

after this time). Subsequently, $[CO_2]$ and $[OH^-]$ decrease slowly along the direction of $\vec{u}$ ($[CO_2]:[OH^-] \approx 1:1$) until equilibrium is achieved.

The temporal course of δOH^- and δCO_2 is explicitly displayed in Fig. 2. The horizontal axis is chosen logarithmic to show the characteristic time scales involved (note that there is no functional dependence such as $\delta OH^- \propto \log(t)$, even though the curve appears to be linear within different intervals). Starting at a value of 0.1 μmol kg^{-1}, δOH^- increases to about 0.6 μmol kg^{-1} within several microseconds (vertical dot-dashed line No. 1, compare τ_3^b). After this time the perturbation in OH^- and CO_2 decrease slowly with the relaxation constant
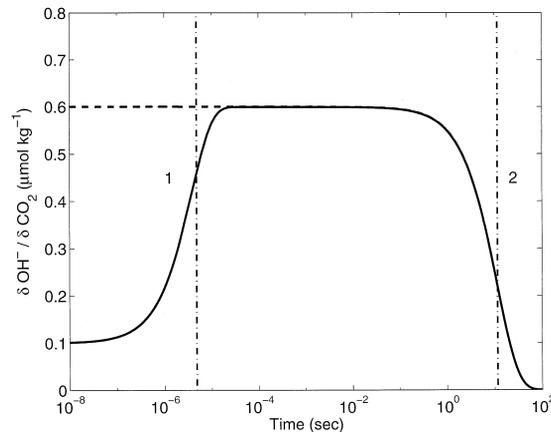
Fig. 2. Temporal development of the perturbation in OH^- (solid line) and CO_2 (dashed line). On a time scale of 10^{-6} s (vertical dot–dashed line No. 1) the perturbation δOH^- increases to six times the initial value (depending on the perturbation in CO_2). Subsequently, δOH^- and δCO_2 decrease to the equilibrium value of zero on a time scale of 10 s (vertical dot–dashed line No. 2).

τ_3^a (vertical dot–dashed line No. 2). In the pH range from 7 to 9 the graphs can excellently be approximated by (see Appendix B):

$$
\begin{aligned}
\delta OH^-(t) &= \delta CO_2^0 \exp(-t/\tau_3^a) + (\delta OH^{-0} - \delta CO_2^0) \exp(-t/\tau_3^b) \\
\delta CO_2(t) &= \delta CO_2^0 \exp(-t/\tau_3^a)
\end{aligned}
\tag{19}
$$

where δOH^{-0} and δCO_2^0 are the initial perturbations in OH^- and CO_2 at $t = 0$. A remarkable result of this analysis is that the perturbation of OH^- first increases abruptly to six times the initial value (depending on the perturbation in CO_2, see Fig. 1). This feature is known as the problem of 'nonnormal' eigenfunctions which arises in other scientific fields such as fluid mechanics or numerical analysis. In cases where a system shows chaotic behavior (most chemical systems are dampened or at most oscillatory) the sudden increase of a perturbation can push the system from a region of regular behavior into a region of chaotic behavior. An example of such a breakdown of order is the transition from a regular flow of a fluid to a turbulent flow at Reynolds numbers far below the critical threshold value (e.g., Trefethen et al., 1993).

The reason for the relaxation of CO_2 and OH^- occurring in a ratio of approximately 1:1 after achieving the 'near-equilibrium' with H_2O is the conservation of charge (alkalinity). The definitions of alkalinity and ΣCO_2 in this particular case are:

$$
Alk = [HCO_3^-] + [OH^-] - [H^+]
$$

$$
\Sigma CO_2 = [CO_2] + [HCO_3^-].
$$

If we assume that OH^- and H^+ are almost in equilibrium it follows that:

$$
[CO_2] \approx \Sigma CO_2 - Alk + [OH^-] - K_w/[OH^-]
$$

with

$$
K_w = \frac{k_{+6}}{k_{-6}} = [H^+][OH^-]
$$

and therefore

$$
\frac{d[CO_2]}{d[OH^-]} \approx 1 + K_w/[OH^-]^2.
$$

Since $K_w/[OH^-]^2$ is in the order of 10^{-4} the ratio of $CO_2:OH^-$ decrease is approximately 1:1.

2.3. The complete chemical system

The complete chemical system (including boron) considered is:

$$
CO_2 + H_2O \underset{k_{-1}}{\overset{k_{+1}}{\rightleftharpoons}} H^+ + HCO_3^-
\tag{20}
$$

$$
CO_2 + OH^- \underset{k_{-4}}{\overset{k_{+4}}{\rightleftharpoons}} HCO_3^-
\tag{21}
$$

$$
CO_3^{2-} + H^+ \underset{k_{-5}}{\overset{k_{+5}}{\rightleftharpoons}} HCO_3^-
\tag{22}
$$

$$
H_2O \underset{k_{-6}}{\overset{k_{+6}}{\rightleftharpoons}} H^+ + OH^-
\tag{23}
$$

$$
B(OH)_3 + H_2O \underset{k_7}{\overset{k_{+7}}{\rightleftharpoons}} B(OH)_4^- + H^+.
\tag{24}
$$
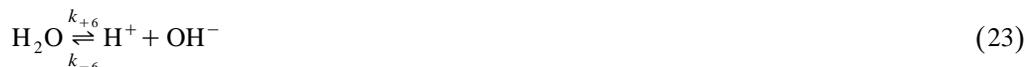
The total dissolved carbon and the alkalinity are defined by:

$$\Sigma CO_2 = [CO_2] + [HCO_3^-] + [CO_3^{2-}]$$

$$Alk = [HCO_3^-] + 2[CO_3^{2-}] + [OH^-] + [B(OH)_4^-] - [H^+].$$

The corresponding set of coupled differential equations (see Appendix A) was integrated numerically by a Runge–Kutta routine of order four with fixed step size (Press et al., 1988). An algorithm with variable step size often gains an advantage. However, it was not useful in this case since even very small deviations from equilibrium in H^+ and OH^- required a time step $< 5 \times 10^{-5}$ s throughout the integration in order to ensure the stability of the algorithm.

The results of the integration are presented in Fig. 3. Starting from equilibrium at pH 8.2 and $[CO_2] = 10.4$ $\mu mol\ kg^{-1}$, CO_2 is increased by a factor of 50% at $t = 0$ to 15.6 $\mu mol\ kg^{-1}$. In addition HCO_3^- and OH^- are decreased and increased, respectively, at $t = 0$ by δCO_2 in order to keep ΣCO_2 and the alkalinity constant. As a response, the pH increases by ca. 0.017 units within several microseconds. Subsequently, CO_2 is converted to HCO_3^- while H^+ is released. The pH decreases and eventually reaches the equilibrium value of 8.2. The time constant for the e-folding time of the calculated decrease in CO_2 is 15.9 s which agrees roughly with the theoretical value of 11.5 s calculated for the simplified system (excluding CO_3^{2-} and boron compounds).

The same results as in Fig. 3 are displayed in Fig. 4 with logarithmic time axis. The decrease of CO_2 is the slowest process and occurs on a time scale of 10 s (Fig. 4a). The concentration of HCO_3^- (CO_3^{2-}) is first decreasing (increasing) after ca. 10^{-2} s and then relaxes to the equilibrium value (Fig. 4b,c). This temporal
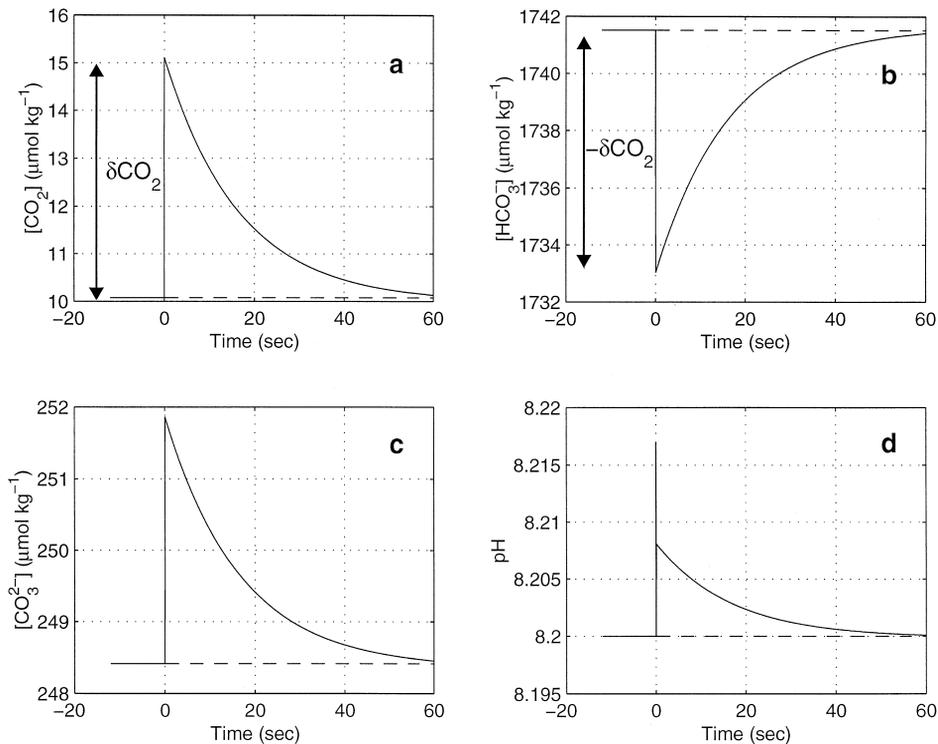
Fig. 3. Numerical results of the relaxation of the carbon species for a perturbation in CO_2 (HCO_3^- at $t = 0$ was reduced by δCO_2 to keep ΣCO_2 constant, whereas OH^- was increased by δCO_2 to keep the alkalinity constant). All chemical species including boron are considered. The dashed lines indicate the equilibrium values of each species which were calculated from ΣCO_2 and alkalinity.
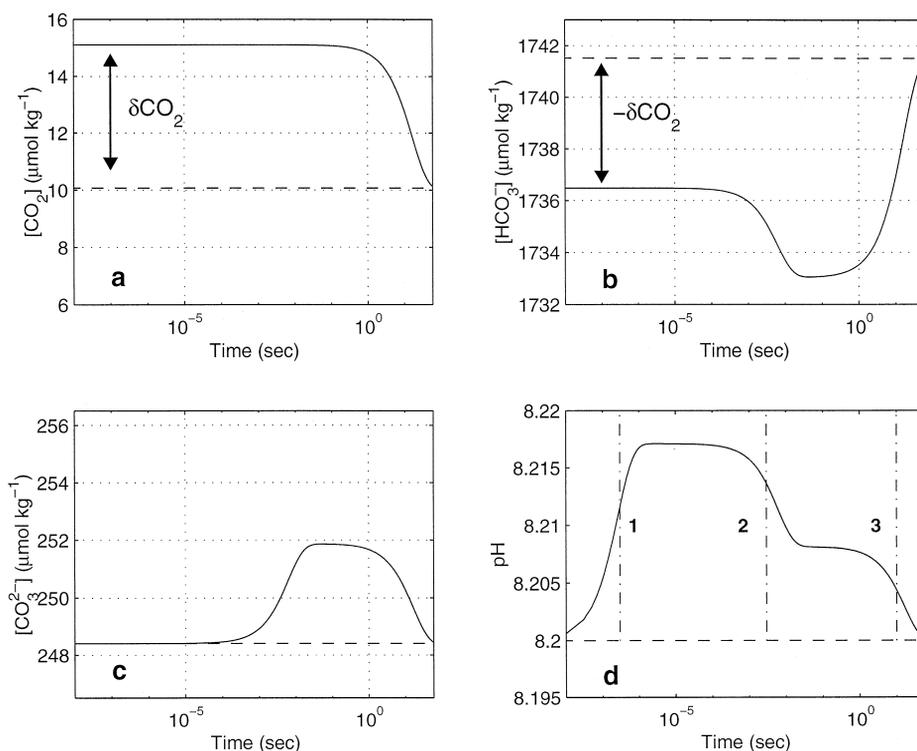
Fig. 4. Same as Fig. 3 with logarithmic time axis. (a) CO_2 decreases on a time scale of 10 s. (b) HCO_3^- and (c) CO_3^- first decrease and increase, respectively, on a time scale of 10^{-2} s and then relax to the equilibrium value on a time scale of 10 s. (d) Since the recombination of OH^- and H^+ is the fastest process (10^{-6} s) the pH exhibits changes on all time scales involved. The vertical dot–dashed lines indicate the different time scales (10^{-6} s, 10^{-2} s, and 10 s).

evolution of the carbon compounds can be explained by examining the pH (Fig. 4d). After ca. 10^{-6} s (see vertical dot-dashed line No. 1 in Fig. 4d) the pH increases due to the recombination of $OH^- + H^+ \rightarrow H_2O$ (OH^- was initially raised and thus H^+ is consumed). Since the pH is higher after that time interval, the carbonate ion concentration shifts to a higher value within 10^{-2} s (vertical dot-dashed line No. 2) while HCO_3^- is consumed and H^+ is produced ($HCO_3^- \rightarrow CO_3^{2-} + H^+$). Finally, CO_2 is converted to HCO_3^- (on a time scale of 10 s) and all components relax to their respective equilibrium values (vertical dot–dashed line No. 3). The outlined analysis of the complete chemical system allows the identification of the involved processes and their characteristic time scales (see Table 1).

Table 1
Reactions and time scale of the carbonate system[a]

Process	Reaction	Time scale
Recombination of H^+ and OH^-	$H_2O \rightleftharpoons H^+ + OH^-$	10^{-6} s
Proton transfer HCO_3^- / CO_3^{2-}	$CO_3^{2-} + H^+ \rightleftharpoons HCO_3^-$	10^{-2} s
Boron compounds	$B(OH)_3 + H_2O \rightleftharpoons B(OH)_4^- + H^+$	10^{-2} s
Conversion CO_2 / HCO_3^-	$CO_2 + H_2O \rightleftharpoons H^+ + HCO_3^-$	10 s
Conversion CO_2 / HCO_3^-	$CO_2 + OH^- \rightleftharpoons HCO_3^-$	10 s

[a]The indicated time scales are characteristic for the respective reactions (note that the times were obtained by the analysis of the complete system, see text).

3. Stable carbon isotopes ^{12}C and ^{13}C

In the previous sections a carbon dioxide system was considered that contained only one species of carbon isotopes. Consequently, the calculated relaxation time reflects the chemical equilibrium of the system. When different isotopes of variable concentrations are present in the solution, the slower reaction rates of the heavier isotopes lead to fractionation effects between the carbon species. For example, the hydration step of CO_2 to HCO_3^- (reaction (20) forward) results in isotopically 'lighter' HCO_3^- of about 13‰. On the other hand, the dehydration step (reaction (20) backward) results in 'lighter' CO_2 of about 22‰ (O'Leary et al., 1992). The difference between the forward and backward reaction equals the equilibrium fractionation between CO_2 and HCO_3^- of about 9‰ (the equilibrium value given by Mook (1986) is 8.97‰ at 25°C). These effects will be included in the formulas given in this section.

3.1. Concept

Including ^{12}C and ^{13}C components, six carbon species have to be considered which can be grouped into two compartments:

<div align="center">

COMPARTMENT 1

$$\boxed{^{12}CO_2 \quad \longleftrightarrow \quad H^{12}CO_3^- \quad \longleftrightarrow \quad ^{12}CO_3^{2-}}$$

COMPARTMENT 2

$$\boxed{^{13}CO_2 \quad \longleftrightarrow \quad H^{13}CO_3^- \quad \longleftrightarrow \quad ^{13}CO_3^{2-}}$$

</div>
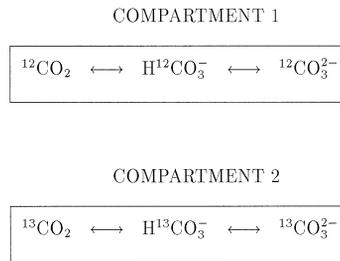
Obviously, there are no direct reactions between the two compartments since each isotope is conserved during reaction. Thus, there are two independent systems, except for the coupling via H^+ and OH^-. Consequently, isotopic equilibrium is achieved when chemical equilibrium is achieved in each compartment.

3.2. The simplified system

Analogously to Section 2.2 we estimate the time to establish equilibrium in a simplified system including the hydration of $^{12}CO_2$, $^{13}CO_2$ and the equilibrium of H_2O (the complete system is again integrated numerically, see Section 3.3). The chemical reactions are:

$$^{12}CO_2 + H_2O \underset{k_{-1}}{\overset{k_{+1}}{\rightleftharpoons}} H^+ + H^{12}CO_3^- \tag{25}$$

$$^{13}CO_2 + H_2O \underset{k'_{-1}}{\overset{k'_{+1}}{\rightleftharpoons}} H^+ + H^{13}CO_3^- \tag{26}$$

$$H_2O \underset{k_{-6}}{\overset{k_{+6}}{\rightleftharpoons}} H^+ + OH^- \tag{27}$$

where the k' are reaction rates of ^{13}C compounds (for values, see Section 3.3). The time constants can again be derived via the eigenvalues of the Jacobian at equilibrium (see Section 2.2). Utilizing the conservation of alkalinity and ΣCO_2, we have:

$$\mathscr{D}|_* = \begin{pmatrix} -1/^{12}\tau_1 & -k_1\left[H^{12}CO_3^-\right]^* & +k_{-1}\left[H^{12}CO_3^-\right]^* \\ -k'_{-1}\left[H^{13}CO_3^-\right]^* & -1/^{13}\tau_1 & +k'_{-1}\left[H^{13}CO_3^-\right]^* \\ +k_{-6}\left[OH^-\right]^* & +k_{-6}\left[OH^-\right]^* & -1/\tau_2 \end{pmatrix} \tag{28}$$

with

$$1/^{12}\tau_1 = k_{+1} + k_{-1}\left([H^+]^* + [H^{12}CO_3^-]^*\right)$$

$$1/^{13}\tau_1 = k'_{+1} + k'_{-1}\left([H^+]^* + [H^{13}CO_3^-]^*\right)$$

$$1/\tau_2 = k_{-6}\left([H^+]^* + [OH^-]^*\right).$$

Since $\mathscr{D}|^*$ is a 3×3 matrix the eigenvalues are the solution of a cubic polynomial. The relaxation times of the system are given by:

$$\tau_a = 28.0\,\text{s}$$

$$\tau_b = 11.5\,\text{s}$$

$$\tau_c = 4.8 \times 10^{-6}\,\text{s}.$$

The characteristic relaxation times of the system correspond to the different mechanisms involved. The shortest time (4.8×10^{-6} s) can be attributed to the recombination of H^+ and OH^-. The second time (11.5 s) is required to establish chemical equilibrium within the ^{12}C compartment (compare the time calculated in Section 2.2 which was 11.5 s). The third time corresponds to the establishment of chemical equilibrium within the ^{13}C compartment and is consequently the time required for isotopic equilibrium. It is emphasized that the slower relaxation of the ^{13}C compounds is a result of the lower concentration in this compartment, rather than a result of different isotopic fractionations of ^{13}C and ^{12}C.

3.3. The complete system including ^{13}C compounds

To calculate the time for isotopic equilibrium in the complete system (including CO_3^{2-} and boron compounds) reactions for the ^{13}C species are added to the set of reactions for the carbon dioxide system (20)–(24). The chemical reactions for the ^{13}C species are:

$$^{13}CO_2 + H_2O \underset{k'_{-1}}{\overset{k'_{+1}}{\rightleftharpoons}} H^+ + H^{13}CO_3^- \tag{29}$$

$$^{13}CO_2 + OH^- \underset{k'_{-4}}{\overset{k'_{+4}}{\rightleftharpoons}} H^{13}CO_3^- \tag{30}$$

$$^{13}CO_3^{2-} + H^+ \underset{k'_{-5}}{\overset{k'_{+5}}{\rightleftharpoons}} H^{13}CO_3^- \tag{31}$$
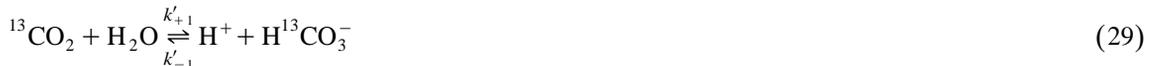
Values for the ratios of reaction rates for the hydration and hydroxylation of CO_2 ((20) and (21) forward) used in the calculations are

$$k'_{+1}/k_{+1} = 0.987 \text{ at } 24°C, \text{ O'Leary et al., 1992} \tag{32}$$

$$k'_{+4}/k_{+4} = 0.989 \text{ O'Leary (pers. comm.)}. \tag{33}$$

Values for the backward reactions (Eqs. (20) and (21)) were calculated from equilibrium fractionation:

$$k'_{-1}/k_{-1} = 0.987 \times \alpha_{(CO_2 - HCO_3^-)} \tag{34}$$

$$k'_{-4}/k_{-4} = 0.989 \times \alpha_{(CO_2 - HCO_3^-)} \tag{35}$$

where $\alpha_{(CO_2 - HCO_3^-)}$ is the equilibrium fractionation between CO_2 and HCO_3^- (Mook, 1986). The fact that there are no data available for k'_{+5}, and k'_{-5} is of minor importance because the equilibrium fractionation between HCO_3^- and CO_3^{2-} is very small (~ 0.5‰). It is much smaller than the fractionation between CO_2 and HCO_3^-

because the proton transfer reaction is several orders of magnitude faster than the carbon–oxygen bond change reaction. The value of k'_{+5} was set to the value of k_{+5} whereas k'_{-5} was calculated from equilibrium fractionation given by Mook (1986).

The set of differential Eqs. (A1), (A2), (A3), (A4), (A5) and (A6) has to be expanded for the equations of the ^{13}C species:

$$\frac{d[^{13}CO_2]}{dt} = +(k'_{-1}[H^+] + k'_{-4})[H^{13}CO_3^-] - (k'_{+1} + k'_{+4}[OH^-])[^{13}CO_2]$$

$$\frac{d[H^{13}CO_3^-]}{dt} = +k'_{+1}[^{13}CO_2] - k'_{-1}[H^+][H^{13}CO_3^-] - k'_{-4}[H^{13}CO_3^-] + k'_{+4}[^{13}CO_2][OH^-] - k'_{-5}[H^{13}CO_3^-] + k'_{+5}[H^+][^{13}CO_3^{2-}]$$

$$\frac{d[^{13}CO_3^{2-}]}{dt} = +k'_{-5}[H^{13}CO_3^-] - k'_{+5}[H^+][^{13}CO_3^{2-}]$$

$$(36)$$

The results of the numerical integration are presented in Fig. 5. The model was initialized with a $\delta^{13}C_{\Sigma CO_2}$ of 2.0‰ and a perturbation in $^{13}CO_2$ which produced an initial $\delta^{13}C$ of CO_2 of ca. 3‰. The concentration of $H^{13}CO_3^-$ was simultaneously decreased by the same amount to keep ΣCO_2 and $\delta^{13}C_{\Sigma CO_2}$ constant. Subsequently, all components relax to reach the equilibrium state. The calculated relaxation time for $\delta^{13}C_{CO_2}$ is 17 s. This is faster than the relaxation time of the simplified system (28 s) mostly due to the inclusion of the additional pathway of the conversion from CO_2 to HCO_3^- $(CO_2 + OH^- \rightarrow HCO_3^-)$ in the complete system.
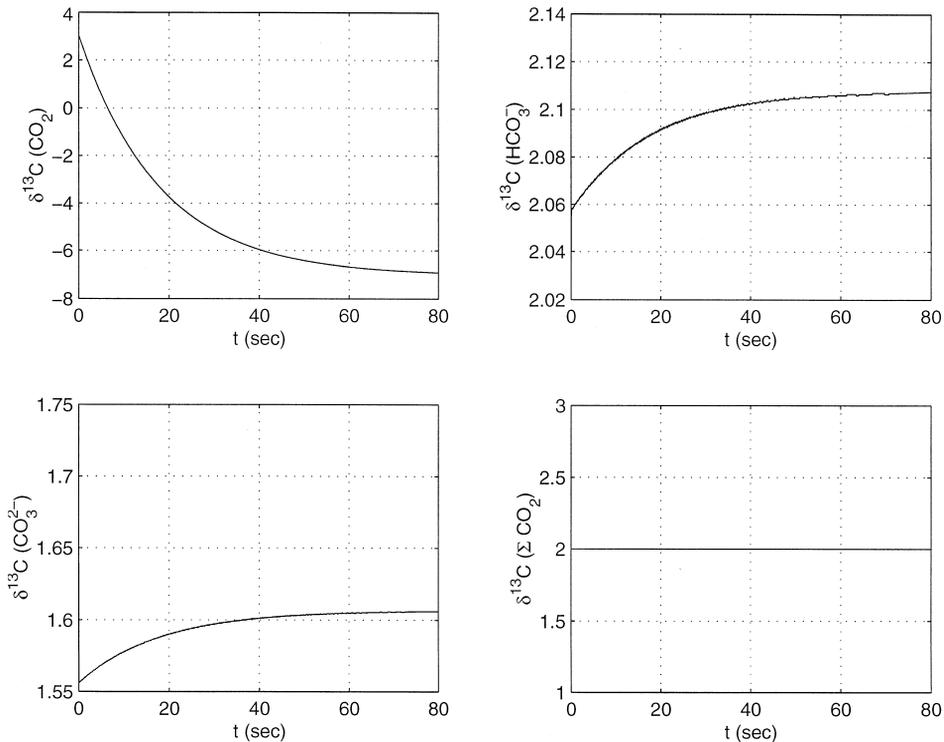
Fig. 5. Numerical results of the relaxation of the complete system (^{13}C and ^{12}C components) and the resulting $\delta^{13}C$ of the carbon species for a perturbation in $^{13}CO_2$ and $H^{13}CO_3^-$. All chemical species including boron are considered. The numerically calculated relaxation time is 17 s.

When this reaction is included in the calculations via the Jacobian at equilibrium, a very similar relaxation time of 17.5 s is obtained (see Section 4).

4. Radiocarbon (^{14}C)

Radiocarbon plays an important role as a tracer for ocean mixing (e.g., Broecker, 1974), in hydrogeological studies (e.g., Mook, 1980; Fontes, 1992) or as a tool for the determination of marine primary production (Strickland and Parsons, 1968). Due to the multiple applications of radiocarbon the radioactivity/concentration of ^{14}C that occurs in the respective investigations may range from 10^1 to 10^{13} dpm g^{-1} C (disintegrations per minute per gram of carbon). This range includes the natural activity of, e.g., atmospheric CO_2 and the measurements of photosynthetic rates. In order to obtain insight into the behavior of the carbonate system under different circumstances the relaxation time for radiocarbon components in seawater will be investigated for various concentrations and pH in this section. The calculations are comparable to the treatment of the stable isotope ^{13}C. However, the relative influence of the fractionation, whether equilibrium or kinetic, is twice as large for ^{14}C as it is for ^{13}C (see Mook (1980) and references therein).

For the purpose of numerical calculations, the amount of radiocarbon in solution which is often expressed in terms of radioactivity has to be converted to a concentration (the following calculation is straightforward; however, it is worth mentioning it since the authors did not find such a calculation in the literature). Radioactivities are usually given in units of Curie (Ci) or Becquerel (Bq). One Becquerel is the amount of radioactive material in which the average number of disintegrations in 1 s is one.

$$1\,\mathrm{Ci} = 3.7 \times 10^{10}\,\mathrm{Bq}\,(\mathrm{disint.\,s}^{-1})$$

From a given activity of a solution (commonly expressed in μCi l^{-1}) and the definition of Ci and Bq the concentration can be calculated. Using the law of radioactive decay the following formula is derived:

$$[c] = A\frac{3.7 \times 10^{10}}{N_A \ln 2}t_{1/2} \approx \frac{A}{62.43}$$

where $[c]$ is the concentration (μmol l^{-1}) of the radiocarbon, A is the activity (μCi l^{-1}), $t_{1/2} = 5730$ years (1.807×10^{11} s) is the half-life of ^{14}C (Mook, 1980), and $N_A = 6.022136 \times 10^{23}$ mol^{-1} is Avogadros constant. Hence, from activities typical for measurements of primary production (120–1200 μCi) follow total concentrations of ^{14}C ($\Sigma^{14}CO_2$) ranging from 2 to 20 μmol l^{-1}.

To determine the time for the relaxation of ^{12}C, ^{13}C, and ^{14}C compounds the following reactions are considered:

$$^{\nu}CO_2 + H_2O \underset{k^{\nu}_{-1}}{\overset{k^{\nu}_{+1}}{\rightleftharpoons}} H^+ + H^{\nu}CO_3^- \tag{37}$$

$$^{\nu}CO_2 + OH^- \underset{k^{\nu}_{-4}}{\overset{k^{\nu}_{+4}}{\rightleftharpoons}} H^{\nu}CO_3^- \tag{38}$$

$$^{\nu}CO_3^{2-} + H^+ \underset{k^{\nu}_{-5}}{\overset{k^{\nu}_{+5}}{\rightleftharpoons}} H^{\nu}CO_3^- \tag{39}$$

$$H_2O \underset{k_{-6}}{\overset{k_{+6}}{\rightleftharpoons}} H^+ + OH^- \tag{40}$$

where ν is 12, 13, and 14. Even though the calculation of the Jacobian (see Section 3.2) is somewhat lengthy (using the conservation of alkalinity and the conservation of the sum of 12-, 13-, and 14-C the Jacobian is a 7×7 matrix), this approach saves time since the subsequent analysis of the system (e.g., parameter studies) by
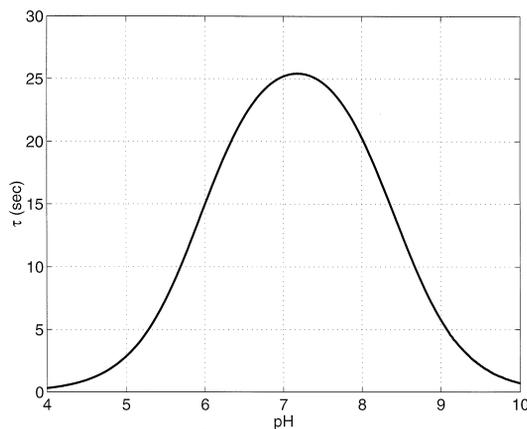
Fig. 6. Relaxation time for chemical and isotopic equilibrium in the carbon dioxide system with respect to the carbon isotopes ^{12}C, ^{13}C, and ^{14}C as a function of pH. The equilibrium is achieved more slowly when the concentrations of the chemical species exhibit similar concentrations (around pH 7).

evaluation of the eigenvalues is fast. Analysis by numerical integration of the differential equations requires appreciably more time since the stiffness of the equations demands a very small time step.

The relaxation time of the system at pH = 8.2, $\Sigma^{14}CO_2 = 2$ and 20 μmol kg^{-1} was 17.467 and 17.463 s, respectively. Thus, the relaxation time is virtually independent of the concentration over this range. The relaxation time τ as a function of pH is presented in Fig. 6. The maximum relaxation time was calculated at pH 7.18 to be 25.4 s. The dependence on pH results from the different paths of conversion of CO_2 to HCO_3^-. At low pH the concentrations of CO_2 and H^+ are high, thus equilibrium with HCO_3^- and OH^- (reaction (37)) is achieved quickly. At high pH the concentrations of HCO_3^- and OH^- are high, thus equilibrium with CO_2 and H^+ (reaction (38)) is achieved quickly. In the pH range where all chemical species exhibit similar concentrations equilibrium is achieved more slowly ($[H^+]^* \approx [OH^-]^*$ around pH 7). This property can also be deduced from the relaxation constants: For instance, τ_2 is of the form $\tau_2 \propto f = 1/([H^+]^* + [OH^-]^*)$ (compare Eq. (8)). For pH 7, $f \approx 0.5 \times 10^7$ kg μmol^{-1}, whereas for pH 4 and pH 10, $f \approx 10^4$ kg μmol^{-1}.

In summary, the time required to establish chemical and isotopic equilibrium in the considered carbon dioxide system is in the order of minutes. The relaxation time is virtually independent of the amount of the radiocarbon present in the solution, when the concentrations range from 2 to 20 μmol kg^{-1} (activity ca. 120–1200 μCi).

5. Summary and conclusions

The presented analysis of the disequilibrium properties of the carbon dioxide system in sea water led to a detailed understanding of the mechanisms which determine the chemical behavior of the system on time scales ranging from microseconds to minutes. The analytical calculations for the simplified system (Section 2.2) showed the essential features of the complete system. Therefore, an expression for the relaxation of a perturbation in $^{12}CO_2$ can be given which is a very good approximation to the exact solution at pH 8.2 (see Appendix B):

$$\delta^{12}CO_2(t) = \delta^{12}CO_2^0 \exp(-t/\tau^a)$$

where $\tau^a = 15.9$ s. The numerical results indicate that the isotopic relaxation time is 17.5 s at pH 8.2 when the carbon isotopes ^{12}C, ^{13}C and ^{14}C are considered. This time is virtually independent of the concentration of the

radiocarbon. However, the relaxation time depends on the pH. It decreases by one order of magnitude when the pH decreases from 7 to 4 or increases from 7 to 10 (Fig. 6).

The measurement of total primary production via addition of radiocarbon yields correct results (with regard to isotopic equilibrium) provided that an equilibration time of ca. 2 min is taken into account (Figs. 5 and 6). Otherwise, the carbon uptake by phytoplankton could be underestimated because the added $H^{14}CO_3^-$ or $^{14}CO_3^{2-}$ has not been converted to $^{14}CO_2$. This property can, on the other hand, be utilized to identify carbon sources for photosynthesis of marine phytoplankton (Korb et al., 1997). The relaxation times derived in this paper can therefore be used to address an important question concerning the inorganic carbon acquisition in marine phytoplankton.

We hope that our results will serve to decide whether equilibrium or disequilibrium properties of the carbonate system should be used. Particularly, it is desired that our approach will help in the development of a time dependent model of carbon and oxygen fractionation in inorganic and biogenic calcite. As proposed by McCrea (1950) and Spero et al. (1997) kinetic isotope effects appear to play a key role in determining the extent of isotopic fractionation during calcite precipitation. It is suggested that disequilibrium of the carbonate chemistry (and isotopes) in the vicinity of the growing crystal is responsible for kinetic isotope effects.

Acknowledgements

Appendix A. Differential equations of the carbon dioxide system (including boron)

$$\frac{d[CO_2]}{dt} = +\left(k_{-1}[H^+] + k_{-4}\right)[HCO_3^-] - \left(k_{+1} + k_{+4}[OH^-]\right)[CO_2] \tag{A1}$$

$$\frac{d[HCO_3^-]}{dt} = +k_{+1}[CO_2] - k_{-1}[H^+][HCO_3^-] - k_{-4}[HCO_3^-] + k_{+4}[CO_2][OH^-]$$
$$- k_{-5}[HCO_3^-] + k_{+5}[H^+][CO_3^{2-}] \tag{A2}$$

$$\frac{d[CO_3^{2-}]}{dt} = +k_{-5}[HCO_3^-] - k_{+5}[H^+][CO_3^{2-}] \tag{A3}$$

$$\frac{d[H^+]}{dt} = +\left(k_{-5} - k_{-1}[H^+]\right)[HCO_3^-] + k_{+1}[CO_2] - k_{+5}[H^+][CO_3^{2-}]$$
$$+ k_{+6} - k_{-6}[H^+][OH^-] + k_{+7}[B(OH)_3] - k_{-7}[H^+]\left[B(OH)_4^-\right] \tag{A4}$$

$$\frac{d[OH^-]}{dt} = +k_{-4}[HCO_3^-] - k_{+4}[CO_2][OH^-] + k_{+6} - k_{-6}[H^+][OH^-] \tag{A5}$$

$$\frac{d[B(OH)_3]}{dt} = -k_{+7}[B(OH)_3] + k_{-7}[H^+]\left[B(OH)_4^-\right] \tag{A6}$$

$$\frac{d[B(OH)_4^-]}{dt} = k_{+7}[B(OH)_3] - k_{-7}[H^+]\left[B(OH)_4^-\right] \tag{A7}$$

Appendix B. Exact solution of the simplified, linearized system

The system (14) is linear and can be solved exactly. It is of the form:

$$\dot{\vec{\delta}} = \mathscr{D}|_* \, \vec{\delta} \tag{B8}$$

Let $\vec{u} = (u_1, u_2)$ and $\vec{v} = (v_1, v_2)$ denote eigenvectors of $\mathscr{D}|^*$ corresponding to eigenvalues λ^a and λ^b. The time development of $\vec{u}$ and $\vec{v}$ is given by:

$$\vec{u}(t) = \vec{u}(0)\exp(\lambda^a t)$$
$$\vec{v}(t) = \vec{v}(0)\exp(\lambda^b t).$$

Since the set of eigenvectors is a basis, every $\vec{\delta}$ can be expressed by:

$$\vec{\delta} = a\vec{u} + b\vec{v}$$

which is also a solution of Eq. (B8). Thus, one has to find the coefficients a and b. They are calculated from the initial condition $\vec{\delta}(t = 0)$. Basically, this procedure represents a transformation of the coordinates of the eigenspace to be the actual coordinates. The result is (replacing $\vec{\delta}$ by $(\delta^{12}CO_2, \delta OH^-)$):

$$\begin{aligned}
\delta OH^-(t) &= \left(\delta^{12}CO_2^0 - \alpha^0\right)\frac{u_2}{u_1}\exp(-t/\tau^a) &+& \quad \alpha^0 \frac{v_2}{v_1}\exp(-t/\tau^b) \\
\delta^{12}CO_2(t) &= \left(\delta^{12}CO_2^0 - \alpha^0\right)\exp(-t/\tau^a) &+& \quad \alpha^0 \exp(-t/\tau^b)
\end{aligned} \tag{B9}$$

with

$$\alpha^0 = \frac{\delta OH^{-0} - \dfrac{u_2}{u_1}\delta^{12}CO_2^0}{\dfrac{v_2}{v_1} - \dfrac{u_2}{u_1}}$$

and

$$\tau^a = -1/\lambda_a$$
$$\tau^b = -1/\lambda_b.$$

Using numerical values of the components of the eigenvectors at pH 8.2, $\vec{u} = (0.7074, 0.7068)$ and $\vec{v} = (-2.88 \times 10^{-4},\ 1 - 4.15 \times 10^{-8})$. One sees that $u_2/u_1 \approx 1$, $|v_2/v_1| \gg u_2/u_1$, and thus $|\delta^{12}CO_2^0| \gg |\alpha^0|$ (these relations are valid in the pH range from 7 to 9). Therefore Eq. (B9) can be approximated by:

$$\begin{aligned}
\delta OH^-(t) &= \delta^{12}CO_2^0 \exp(-t/\tau^a) + \left(\delta OH^{-0} - \delta^{12}CO_2^0\right)\exp(-t/\tau^b) \\
\delta^{12}CO_2(t) &= \delta^{12}CO_2^0 \exp(-t/\tau^a)
\end{aligned} \tag{B10}$$

which was given in Section 2.2.1 (compare Eq. (19)).

References

Archer, D., Maier-Reimer, E., 1994. Effect of deep-sea sedimentary calcite preservation on atmospheric CO_2 concentrations. Nature 367, 260–263.

Atkins, P.W., 1990. Physical Chemistry. Oxford Univ. Press, pp. 794–796.

Broecker, W.S., 1974. Chemical Oceanography. Harcourt, Brace Jovanovich, New York, pp. 59–73.

Broecker, W.S., Peng, T.-H., 1993. What caused the glacial to interglacial CO_2 change? In: Heimann, M. (Ed.), The Global Carbon Cycle. NATO ASI Series I: Global Environmental Change, Vol. 15, Springer, Berlin, pp. 95–115.

DOE, 1994. Handbook of methods for the analysis of the various parameters of the carbon dioxide system in sea water; version 2. In: Dickson, A.G., Goyet C. (Eds.), ORNL/CDIAC-74.

Emerson, S., 1995. Enhanced transport of carbon dioxide during gas exchange. In: Jähne, B., Monahan E.C. (Eds.), Air–Water Gas Transfer. AEON Verlag & Studio, Hanau, pp. 23–35.

Fontes, J.Ch., 1992. Chemical and isotopic constraints on ^{14}C dating of groundwater. In: Taylor, R.E., Long, A., Kra, R.S. (Eds.), Radiocarbon after four decades. Springer, New York, pp. 242–261.

Kim, S.-T., O'Neil, J.R., 1997. Equilibrium and nonequilibrium oxygen isotope effects in synthetic carbonates. Geochim. Cosmochim. Acta 61, 3461–3475.

Korb, R.E., Saville, P.J., Johnston, A.M., Raven, J.A., 1997. Sources of inorganic carbon for photosynthesis by three species of marine diatom. J. Phycol. 33, 433–440.

Lazier, J.R.N., Mann, K.H., 1989. Turbulence and the diffusive layers around small organisms. Deep-Sea Res. 36, 1721–1733.

Lehman, J.T., 1978. Enhanced transport of inorganic carbon into algal cells and its implication for biological fixation of carbon. J. Phycol. 14, 33–42.

Maier-Reimer, E., Hasselmann, K., 1987. Transport and storage of CO_2 in the ocean - an inorganic ocean-circulation carbon cycle model. Climate Dynamics 2, 63–90.

McCrea, 1950. On the chemistry of carbonates and a paleotemperature scale. J. Chem. Phys. 18 (6), 849–857.

Millero, F.J., 1995. Thermodynamics of the carbon dioxide system in the oceans. Geochim. Cosmochim. Acta 59, 661–677.

Mook, W.G., 1980. Carbon-14 in hydrogeological studies. In: Fritz, P., Fontes, J.Ch. (Eds.), Handbook of Environmental Isotope Geochemistry 1. Elsevier, Amsterdam, pp. 49–74.

Mook, W.G., 1986. [13]C in atmospheric CO_2. Netherlands Journal of Sea Research 20, 211–223.

O'Leary, M.H., Madhavan, S., Paneth, P., 1992. Physical and chemical basis of carbon isotope fractionation in plants. Plant, Cell and Environment 15, 1099–1104.

Press, W.H., Flannery, B.P., Teukolsky, S.A., Vetterling, W.T., 1988. Numerical Recipes in C. Cambridge Univ. Press, New York, pp. 609–621.

Siegenthaler, U., 1993. Modelling the present-day oceanic carbon cycle. In: Heimann, M. (Ed.), The Global Carbon Cycle, NATO ASI Series I: Global Environmental Change, Vol. 15. Springer, Berlin, pp. 367–395.

Spero, H.J., Bijma, J., Lea, D.W., Bemis, B.E., 1997. Effect of seawater carbonate concentration on foraminiferal carbon and oxygen isotopes. Nature 390, 497–500.

Strickland, J.D.H., Parsons, T.R., 1968. In: Stevenson, J.C. (Ed.), A Practical Handbook of Sea Water Analysis. Queen's Printer, Ottawa, pp. 267–278.

Stumm, W., Morgan, J.J., 1996. Aquatic Chemistry, 3rd edn., Wiley, New York.

Trefethen, L.N., Trefethen, A.E., Reddy, S.C., Driscoll, T.A., 1993. Hydrodynamic stability without eigenvalues. Science 261, 578–584.

Usdowski, E., 1982. Reactions and equilibria in the systems CO_2–H_2O and $CaCO_3$–CO_2–H_2O (0°–50°C). N. Jb. Miner. Abh., 148–171.

Wolf-Gladrow, D.A., Riebesell, U., 1997. Diffusion and reactions in the vicinity of plankton: a refined model for inorganic carbon transport. Mar. Chem. 59, 17–34.

Wolf-Gladrow, D.A., Bijma, J., Zeebe, R.E., 1999. Model simulation of the carbonate system in the microenvironment of symbiont bearing foraminifera. Mar. Chem. 64, 181–198.

Zeebe, R.E., Bijma, J., Wolf-Gladrow, D.A., 1999. A diffusion-reaction model of carbon isotope fractionation in foraminifera. Mar. Chem. 64, 199–227.